Arrangement of Tubulin Subunits and Microtubule-associated Proteins in the Central-Pair Microtubule Apparatus of Squid (*Loligo pealei*) Sperm Flagella

R. W. LINCK, G. E. OLSON, AND G. L. LANGEVIN
Department of Anatomy, Harvard Medical School, Boston, Massachusettts 02115, and the Department of Anatomy, Vanderbilt University, Nashville, Tennessee 37232

ABSTRACT This study provides a comprehensive, high-resolution structural analysis of the central-pair microtubule apparatus of sperm flagella. It describes the arrangement of several microtubule-associated "sheath" components and suggests, contrary to previous thinking, that microtubules are structurally asymmetric. The two microtubules of the central pair are different in several respects: the C_2 tubule bears a single row of 18-nm-long sheath projections with an axial periodicity of 16 nm, whereas the C_1 tubule possesses rows of 9-nm globular sheath components with an axial repeat of 32 nm. The lumen of the C_2 tubule always appears completely filled with electron-dense material; that of the C_1 tubule is frequently hollow. The C_2 tubule also possesses a series of beaded chains arranged around the microtubule; the beaded chains are composed of globular subunits 7.5–10 nm in diameter and appear to function in the pairing of the C_1 and C_2 tubules. These findings indicate: that the beaded chains are not helical, but assume the form of lock washers arranged with a 16-nm axial periodicity on the microtubule; and that the lattice of tubulin dimers in the C_2 tubule is not helically symmetric, but that there are seams between certain pairs of protofilaments. Proposed lattice models predict that, because of these seams, central pair and perhaps all singlet microtubules may contain a ribbon of 2–5 protofilaments that are resistant to solubilization; these models are supported by the results of the accompanying paper (R. W. Linck, and G. L. Langevin. 1981. *J. Cell Biol.* 89: 323–337).

A pair of singlet microtubules is located within the "9 + 2" ciliary and flagellar axoneme and is commonly referred to as the "central pair." It has been shown that the central pair plays an important role in the regulation of axonemal motility (58, 79, 82). To define the molecular basis of this regulation, we have investigated the ultrastructure of the central-pair microtubules from squid sperm flagella. We were also interested in determining what features these flagellar singlet microtubules might have in common with other cytoplasmic microtubules.

Aside from their role in ciliary and flagellar motility, a potentially important feature of the central pair microtubules, is that they resemble cytoplasmic microtubules more than do the extensively studied peripheral doublet microtubules (6, 11, 21, 35, 39, 42, 69, 80, 81). The central tubules are true singlet microtubules composed of 13 protofilaments (75). Although the central tubules *in situ* are cold-stable, in many species they are easily solubilized by low ionic strength, divalent cation-free solvents (25), and the resulting soluble central-pair tubulin binds colchicine stoichiometrically (67). Central-pair tubules also possess several different structural components that bind with 16- and 32-nm axial periodicities, in contrast to the 24-nm dynein arm spacing and more complex spacings of the radial spokes of the outer doublet microtubules (41). In this regard, central tubules resemble brain microtubules that possess high molecular weight, microtubule-associated proteins with axial spacings of 32 (34, 54) or 96 nm (4), as well as microtubules of undulating axostyles that possess a dynein-like ATPase (53) and cross-bridge arms with axial spacings of 16 nm (51, 53, 83).

Importantly, the arrangement or lattice of tubulin dimers

THE JOURNAL OF CELL BIOLOGY · VOLUME 89 MAY 1981 309–322

has not been unambiguously determined for central-pair microtubules nor for any cytoplasmic single microtubules, although this has been investigated (15). The tubulin dimer lattices have been determined for the A and B tubules of flagellar doublet microtubules (6, 42), and most investigators have assumed that the dimer lattice of A tubules is true for all single microtubules; however, there is no direct proof. In the present study we characterize, in one species, the arrangement of various microtubule-associated structures on the central-pair apparatus. We also analyzed the relationship of these components to the surface lattice of the microtubule and propose new models for the subunit arrangement of tubulin in the microtubule. In addition, the proposed models of singlet microtubules are supported by the results of the accompanying paper (44).

MATERIALS AND METHODS

Animal and Spermatophore Collection

Squid, *Loligo pealei*, were obtained from the Marine Biological Laboratory, Woods Hole, Mass. To collect sperm, we decapitated squid and cut along the midventral axis of the body, avoiding the ink sac. The spermatophoric sac (18), containing anywhere from ten to several hundred spermatophores, was dissected out and placed in a beaker on ice. We preferred to try to keep the duct intact to facilitate collection of the small, white spermatophores (0.5 × 5 mm).

Sperm Fractionation Procedures

Demembranated sperm were prepared as follows: 10–25 g of packed spermatophores (from ~25–50 male squid) were minced and extracted in filtered seawater to which was added 0.1 mM EDTA. The sperm suspension was then filtered through cheesecloth and pelleted in 40-ml tubes at 2,000 g_{avg} for 5 min. The pellets of sperm were resuspended in an equal volume of demembranating solution, containing 1% Triton X-100, 0.15 M KCl, 5 mM $MgSO_4$, 0.5 mM EDTA, 10 mM Tris, 1 mM ATP, and 1 mM dithiothreitol (DTT), pH 8.3. This and all subsequent steps were performed at 4°C. Enough demembranating solution was then added to bring the final volume to 10 times the original spermatophore volume. The sperm suspension was stirred slowly for 20 min and then centrifuged in 40-ml tubes at 2,500 g_{avg} for 8 min. The supernates were carefully aspirated and the sperm pellets resuspended in demembranating solution and recentrifuged. The demembranated sperm were washed twice by resuspension and centrifugation in storage solution of the same ionic composition as the demembranating solution, except for the absence of Triton. The demembranated, washed sperm were stored as pellets on ice for use later.

The central-pair microtubules were isolated for these studies by the following procedure: the demembranated, washed sperm pellets described above were resuspended in ~10 vol of high-salt solution containing 0.5 M KCl, 10 mM Tris, 5 mM EDTA, 1 mM ATP, and 1 mM DTT, pH 8, extracted for 30 min on ice, and centrifuged in 10- to 40-ml tubes at 2,500 g_{avg} for 5 min. The pellet consisted of extracted sperm (sperm heads with attached, frayed tail fibers); the supernate containing isolated central-pair microtubules and soluble protein appeared clear. The suspension of central pairs either was used directly for negative staining or pelleted at 32,000 g_{avg} for 45 min. Several other salt solutions were also tried for their ability to selectively remove the central pair. Such solutions included different (lower) KCl concentrations, different pH's (6 vs. 8), replacement of EDTA with 1 mM $MgSO_4$, and elimination of ATP. All solutions worked as long as the KCl concentration was 0.3 M or greater. 10 g of packed sperm yielded ~1 mg of purified central-pair microtubules.

Squid sperm flagella were isolated as follows: live sperm in the seawater filtrate were homogenized in a 50-ml Dounce homogenizer (Kontes Co., Vineland, N. J.), using 100 down strokes of the plunger. 5-ml aliquots of homogenized sperm were layered on step gradients of 10 (25 ml) and 60% (10 ml) sucrose, containing 0.15 M KCl, 10 mM Tris, 5 mM $MgSO_4$, 0.5 mM EDTA, 1 mM ATP, and 1 mM DTT, pH 8, and centrifuged in a Sorvall HB swinging-bucket rotor at 5,500 rpm (5,000 g_{avg}) for 15 min (DuPont Instruments = Sorvall, DuPont Co., Newtown Conn.). The heads and intact sperm pelleted to the bottom of the tubes, whereas the flagella and some contaminating heads layered between the 10 and 60% sucrose layers. The flagella were siphoned off and repurified on a second set of gradients in the same manner. The isolated flagella were pure as judged by phase-contrast microscopy and were subsequently demembranated by two cycles of washing in demembranating solution as described above for whole sperm, except that centrifugation was done at 10,000 g_{avg} for 10 min.

Electron Microscopy

Material for thin sections was fixed, except as noted, for 1 h in 3% glutaraldehyde, 0.15 M KCl, 10 mM sodium phosphate, and 4 mM $MgSO_4$, pH 7.2, washed with 10 mM sodium phosphate, pH 6.0, and postfixed for 30 min with 1% osmium tetroxide in 10 mM sodium phosphate, pH 6.0.

Fixed materials were dehydrated with a graded series of ethanol, washed with propylene oxide, and embedded in Epon 812. All steps of fixation and dehydration were performed at 4°C.

For negative staining, carbon film grids were prepared by evaporation of carbon onto Formvar membranes and subsequent removal of the Formvar with 1,2-dichloroethane. One drop of sample was applied to the carbon film, followed by three drops of axoneme storage solution, followed by seven drops of 1% uranyl acetate, which was drawn off and the excess allowed to dry. Electron micrographs of negatively stained material were obtained with a JEOL 100B instrument operated at 80–100 kV.

Image Analysis

Optical diffraction and filtering of electron microscope images were carried out according to the method of Klug and DeRosier (36), as described in detail by Olson and Linck (56).

Polyacrylamide Gel Electrophoresis

Sodium dodecyl sulfate-polyacrylamide gel electrophoresis was carried out according to the procedures of Bryan (12) and Stephens (68), using a 6% acrylamide–0.16% *bis*-acrylamide running gel with no stacking gel. The gels were stained according to the procedure of Fairbanks et al. (20).

RESULTS

Isolation of Central-Pair Microtubules

Following demembranation, squid sperm flagella remain firmly attached to the sperm head as judged by phase-contrast microscopy (data not shown). Electron micrographs of thin sections (Fig. 1) indicate that the demembranated flagellar axonemes are intact or partially frayed; nevertheless, even in the cases of the frayed axonemes, the central-pair microtubules usually remain associated with the spokes of the adjoining doublet microtubules. The demembranated flagella display a typical 9 + 2 arrangement (Fig. 3) with accompanying pairs of dynein arms and radial spokes. An accessory fiber is attached to each doublet microtubule, as described earlier in molluscs by Anderson and Personne (7). In negative stain (data not shown), the accessory fiber and doublet tubule are seen to be attached firmly to one another throughout their length. The accessory fibers gradually taper from base to tip and terminate before the ends of the doublet tubules. At their proximal ends, the accessory fibers retain their membrane attachments (Fig. 3 *d*), as recently described by Olson and Linck (57).

The central-pair microtubules are frequently oriented within the axoneme such that a plane passing through the two tubules is perpendicular to a ray from the center of the axoneme to outer doublet tubule 1 (1; see Fig. 3 *b*). According to Afzelius (1) and others (24, 56, 64, 79), the oppositely directed ray passes between outer doublets 5 and 6, marked by a so-called 5–6 bridge. The existence of a 5–6 bridge in squid sperm remains uncertain. However, because some evidence indicates that the central pair may actually rotate within the nine-fold axoneme (58, 74), it may be impossible to establish here the absolute identity of the outer nine doublets. Thus the only unequivocal criterion for orientation of squid flagellar axonemes, in the absence of a 5–6 bridge, is the asymmetry of the central pair; i.e., one central microtubule, the C_2 tubule, is invariably solid, with no lumen, and possesses a single 18-nm-long projection, whereas the C_1 tubule is frequently, though not always, hollow. Further discussion of the central-pair microtubule apparatus

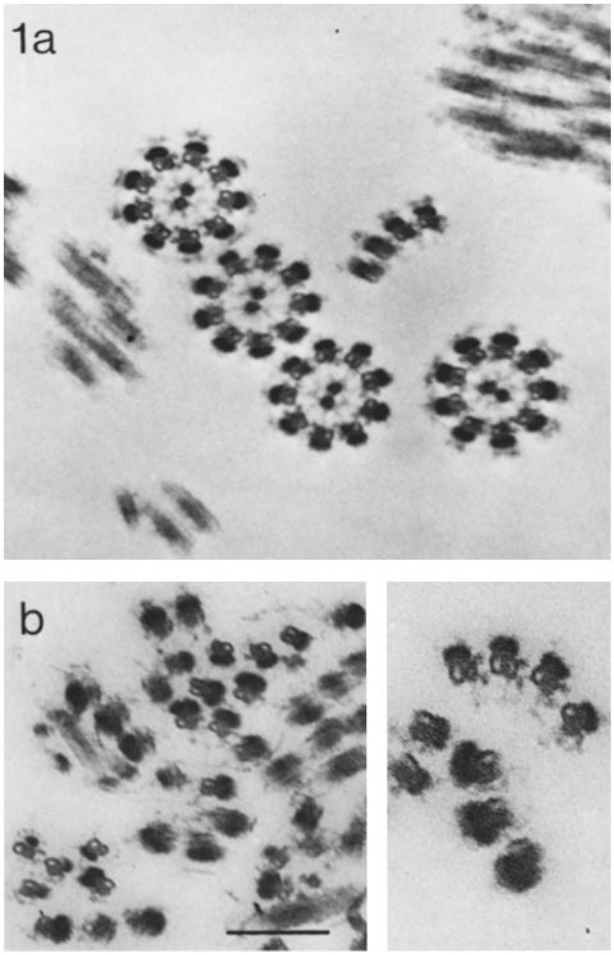

FIGURE 1 *a:* Demembranated squid sperm flagella display a relatively intact 9 + 2 appearance. *b:* A low-speed pellet of squid sperm, after demembranation and extraction with 0.5 M. KCl, shows the disrupted appearance of the axoneme and the absence of central pair. *Insert* of *b* shows continued presence of dynein arms associated with salt-extracted doublet tubules. Bar: for *a* and *b* = 200 nm; for *Insert* = 120 nm.

will be deferred until later.

Extraction of demembranated sperm with high-salt solution (0.5 M KCl, 10 mM Tris, pH 8.3) causes complete fraying of the axonemes, as determined by light and electron microscopy (Fig. 1 *b*), and a concomitant release of the central pair. In the high-salt-extracted sperm, both inner and outer dynein arms and radial spokes remain attached to the frayed doublet tubules, and the latter to the accessory fibers. Central-pair microtubules are not seen in the low-speed, 2,000 *g* pellet of high-salt-extracted sperm. The doublet tubules and accessory fibers remain attached to the sperm heads, facilitating their removal by low-speed centrifugation, leaving the central pair in the supernate.

A thin section of a high-speed, 32,000 *g* pellet of the purified central pair is shown in Fig. 2. High magnification cross-section images are displayed in Fig. 4. Although the purity of the central pair varied from preparation to preparation, a purity of 95%, as judged by EM or by SDS gels (Fig. 5), could be obtained with little difficulty. SDS-polyacrylamide gels reveal the purity and protein composition of the isolated central pair: because the accessory fibers represent nearly half of the mass of the demembranated flagella, they undoubtedly account for the second most abundant flagellar protein, parergin (8), with a molecular weight of ~37,000 daltons, relative to the most abundant proteins α- and β-tubulin (Fig. 5). Because the accessory fibers remain firmly attached to the doublet tubules, parergin does not appear in the isolated central pair. Thus, its absence is a useful criterion for the purity of the central-pair preparation. Central-pair preparations contain, in addition to tubulin (which accounts for ~75% of the protein), at least five other proteins in significantly greater amounts than in flagellar axonemes. Dynein, ~350,000 daltons (27), and other high molecular weight, microtubule-associated proteins are present in small quantities in the central-pair preparations, although their relation to the central-pair microtubules is not yet clear. The numerous other nontubulin bands very likely have their origin in the equally numerous fine-structural elements found associated with the central pair microtubules (see below).

Ultrastructure of the Central-Pair Microtubule Apparatus in Thin Section

In thin section, the two individual microtubules of the central-pair apparatus possess several structurally distinguishing

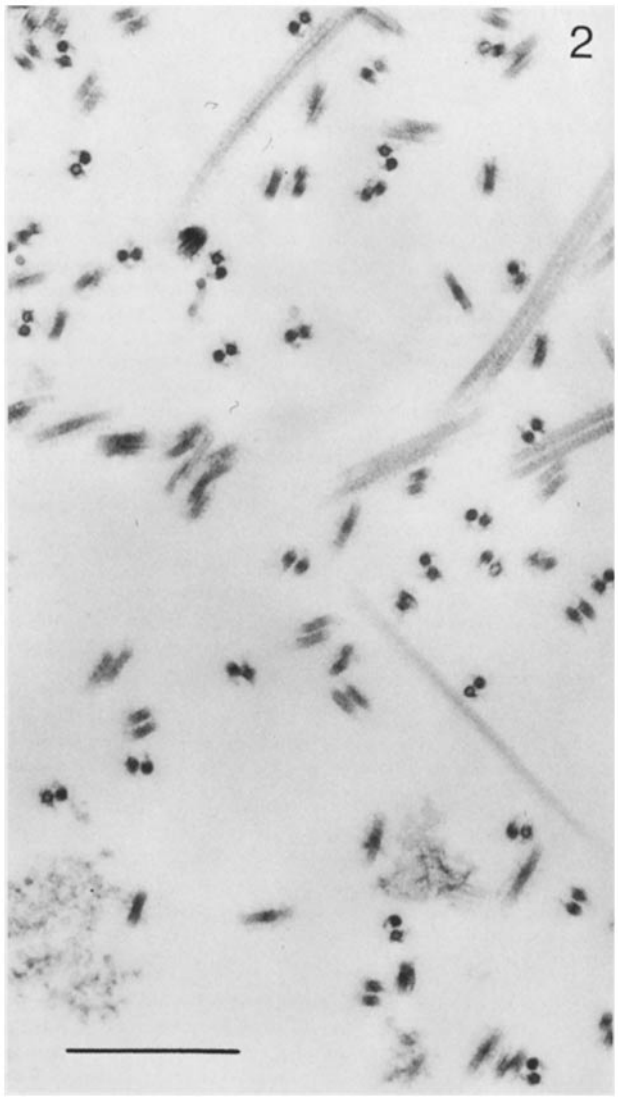

FIGURE 2 Thin section from pellet of isolated squid sperm central-pair of microtubule apparatus. Note the purity relative to the few contaminating doublet-tubule dense fibers and some flocculent material. Bar, 0.5 μm.

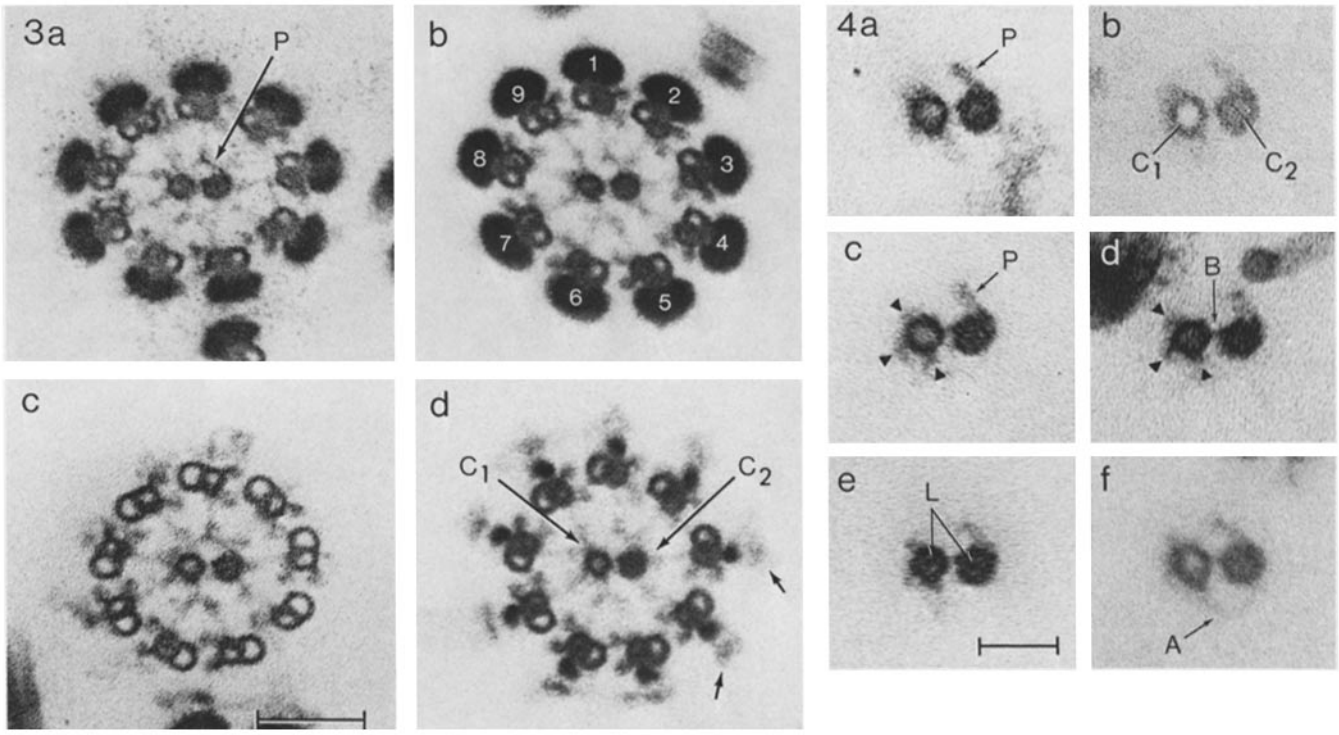

FIGURE 3 Cross sections of demembranated squid sperm flagella. The 9 + 2 axonemes are viewed in their clockwise enantiomorphic form (dynein arms directed clockwise) and oriented with the C_1 central microtubule on the left and the C_2 tubule on the right. The C_1 tubule is frequently hollow, whereas the lumen of the C_2 tubule is filled with dense material. The C_2-tubule possesses a single 18-nm-long projection (*P*) emanating from its upper surface and projecting toward the spoke head of the upper doublet tubule. In all cases shown, a line perpendicular to the coaxial plane of the central tubules bisects the upper doublet tubule designated as 1 (Fig. 3 *b*); however, in light of the possible rotation of the central pair within the axoneme (58, 74), the numbering of the outer nine doublets may be arbitrary. Other features include: dense fibers (numbered in Fig. 3 *b*) associated with their respective doublet tubules and membrane attachment material (arrows) remaining associated with each dense fiber. Bar, 100 nm.

FIGURE 4 Cross sections of isolated central-pair microtubule apparatus are oriented with the C_1 tubule on the left, the C_2 tubule on the right, and the projection *P* up, as in Fig. 3. The lumen of the C_2 tubule is invariably solid, whereas that of the C_1 tubule is frequently, but not always hollow. The C_1 and C_2 tubules occasionally show a 6- to 7-nm subunit *L* in the center of their lumens (*e*). The C_2 tubule possesses a single projection *P*; the C_1 tubule possesses three structural elements, 5 × 8 nm (▲), attached at characteristic points around its outer surface. The two central tubules are occasionally connected at their closest points by a 7- to 10-nm-long bridge *B* (*d*) and/or by a thick filamentous arch *A* (*f*). Bar, 75 nm.

features. First and most notable, the lumen of one of the two microtubules, the C_2 tubule, is always filled with dense material, whereas that of the C_1 tubule is frequently but not always hollow (cf. Figs. 3 and 4). In numerous cases where the C_1, C_2, or both central tubules appear filled, a 7 nm diameter structure appears in the center of the lumen (Figs. 3*c*, 4*e*). Second, the solid C_2 tubule possesses a single prominent projection measuring 5 × 18 nm. It appears in cross section to be attached at an angle of 40–55° to a line through both central tubules. Third, a bridging element 6–9 nm long connects the two tubules at their closest points. It is difficult to measure the length of this bridge accurately, due to the variable wall thicknesses of the microtubules, but it is not more than 10 nm. The nature of this bridge will be discussed in more detail below (in The Basis of Pairing). Finally, the usually hollow C_1 tubule possesses three structural elements associated with its outer surface: these structures, ~5 × 8 nm, appear around the circumference of the tubule wall at 130°, 205°, and 290°, measured in a counterclockwise fashion from the central-pair bridge (Fig. 4*c* and *d*). Some of these features are observed in cross sections of the demembranated axonemes (Fig. 3), such as the hollowness of the C_1 tubule and the 18-nm-long projections of the C_2 tubule. The projection is seen to make contact at its tip with the radial spoke head of the doublet tubule designated as 1. The structures on the C_1 tubule are seen less clearly in the axonemes, but they are in close proximity to the radial spokes of doublets 6, 7, 8, and 9. Occasionally, thin filamentous material connects the tip of the C_2 projection to the C_1 tubule (Fig. 4*f*) and the two central tubules to one another by means of an arch (Fig. 4*f*) on the other side of the axoneme; it is not clear whether these thin filaments are real or artifact.

Ultrastructure of Central Pair in Negative Stain

A greater understanding of the three-dimensional organization of the central-pair microtubule apparatus is gained from negative-stain images (Fig. 6–12). As with the thin-section analysis, a comparison of negatively stained preparations of isolated central pair and demembranated flagellar axonemes indicates that the isolated central pair is indistinguishable from the central pair of flagella before high-salt extraction; however, use of isolated central pairs has greatly facilitated the study of their structure.

After negative staining, isolated central-pair apparatus either remain intact (Figs. 6, 9, 10, and 12) or dissociate into their two tubules (Figs. 7 and 8). In the latter case, the dissociation

must be a result of the uranyl acetate (pH 4.5) or surface tension of the carbon film, because cross sections of fixed material (Figs. 2 and 4) indicate that the central tubules remain paired after isolation. Thus, the high-salt treatment used in the isolation is not responsible for the dissociation apparent in negative stain.

The microtubules of the intact central pair appear to be joined tightly along their length (Fig. 6). In some cases, the walls of the two tubules appear to be in direct contact, although a gap of 6–8 nm is sometimes observed. The apparent distance between tubules varies with the tilt of the central pair on the carbon film, but a gap of 6–8 nm is in agreement with thin-section analysis (Figs. 3 and 4). Both tubules of the central pair are coated with a complex set of structures, as illustrated in Fig. 9, wherein areas of coated microtubules are continuous with areas that are stripped clean, revealing the presumably bare walls of the microtubules. As in cross section, however, the two central tubules are different, and for clarity they will be described separately. The numbering system of the central-pair tubules follows our previous convention (56). (See Discussion.)

The C_2 Central Microtubule

The C_2 tubule is more smoothly and evenly stained than the C_1 tubule that is heavily mottled. This appearance is true whether the tubules of the central pair are intact (Fig. 6) or dissociated (Figs. 7 and 8). The C_2 tubule possesses a single row of prominent structures repeating at 16 nm axially (Figs. 6 and 7). The row of projections is best seen in dissociated central-pair apparatus (Fig. 7): in negative stain the projections are seen to measure 5 × 18 nm with an axial repeat of 16 nm and appear to be connected to one another at their tips by a thin filament. The projections are entirely different from the radial spokes with respect to their size and axial repeats. These projections correspond to those described, in thin section, emanating from the C_2 tubule and directed toward the radial spoke of doublet tubule 1.

Another feature of the C_2 tubule is illustrated in Fig. 9: in addition to the more prominent projections (that are perpendicular to the plane of the figure), a series of smaller dots are associated with the outer (right-hand) edge of the C_2 tubule. These dots also repeat at 16 nm axially, but are slightly out of register with the projections by ~5 nm. Such small periodic components are observed even when the projections are not preserved or contrasted by uranyl acetate (Figs. 10 and 11). This 16-nm periodicity appears to arise from a striated arrangement of globular subunits arranged obliquely around the outside of the microtubule as revealed in Fig. 11. Optical diffraction patterns of the C_2 tubule show off-meridional reflections on the 16-nm^{-1} layer line and orders thereof. Strong equatorial reflections occur at 5 and 7.5–10 nm^{-1}, the latter reflections being indicative of a helical or helixlike arrangement of globular subunits, rather than a helically wound fiber. Several specimens tended to be stained more heavily on one side than the other as judged by the optical transforms of their images (e.g., Fig. 11 *a* and *c*). Optical reconstruction of such predominately one-sided images was performed using layer-line-filtering techniques (inclusion of all signal and noise on the 16-, 8-, and 4-nm^{-1} layer line, the origin and the prominent equatorial reflections). A comparison of the optical transforms and layer-line-filtered images with the surface lattice of the microtubule suggested a tentative lattice indexing of the 16- and 8-

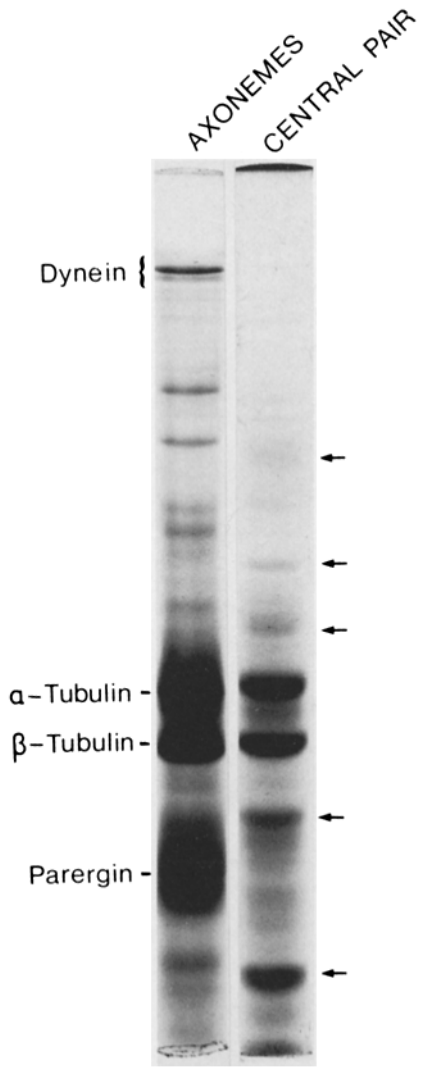

FIGURE 5 SDS-polyacrylamide gels of purified squid sperm flagella (demembranated) and isolated central pair. Parergin is the principal structural protein of the accessory dense fibers (8); its absence in the gel on the right is an indication of the purity of the central pair preparation. Five polypeptides (arrows) are enhanced in the central pair preparation relative to their amounts in the axoneme.

nm^{-1} layer lines and 10-nm^{-1} equatorial reflections (Fig. 11 *c*). Optical reconstructions were then prepared on the basis of this lattice, one of which is presented in Fig. 11 *b*; the lattice-filtered and layer-line-filtered images were similar, although the former was clearer. On close inspection, the details of the filtered image (Fig. 11 *b*) can be seen in the original image (Fig. 11 *a*).

These results are consistent with a structure (Figs. 11 *b* and 13) in which 7.5–10 nm diameter globules are wound as a beaded chain around the microtubule, forming a unit cell of dimensions (7.5–10) × 16 nm^{-1}. The images indicate that the beaded chain must approximate a one- or two-start helix, although the exact pitch has not yet been determined. A consideration of the microtubule lattice suggests that it may not be possible to superimpose on it, with perfect helical symmetry, a 16-nm helix (see Fig. 13 *a* and Discussion); these data, therefore, raise the possibility that the microtubule lattice is not helically symmetrical and that the beaded chains are arranged in the manner of dislocated helices or lock washers.

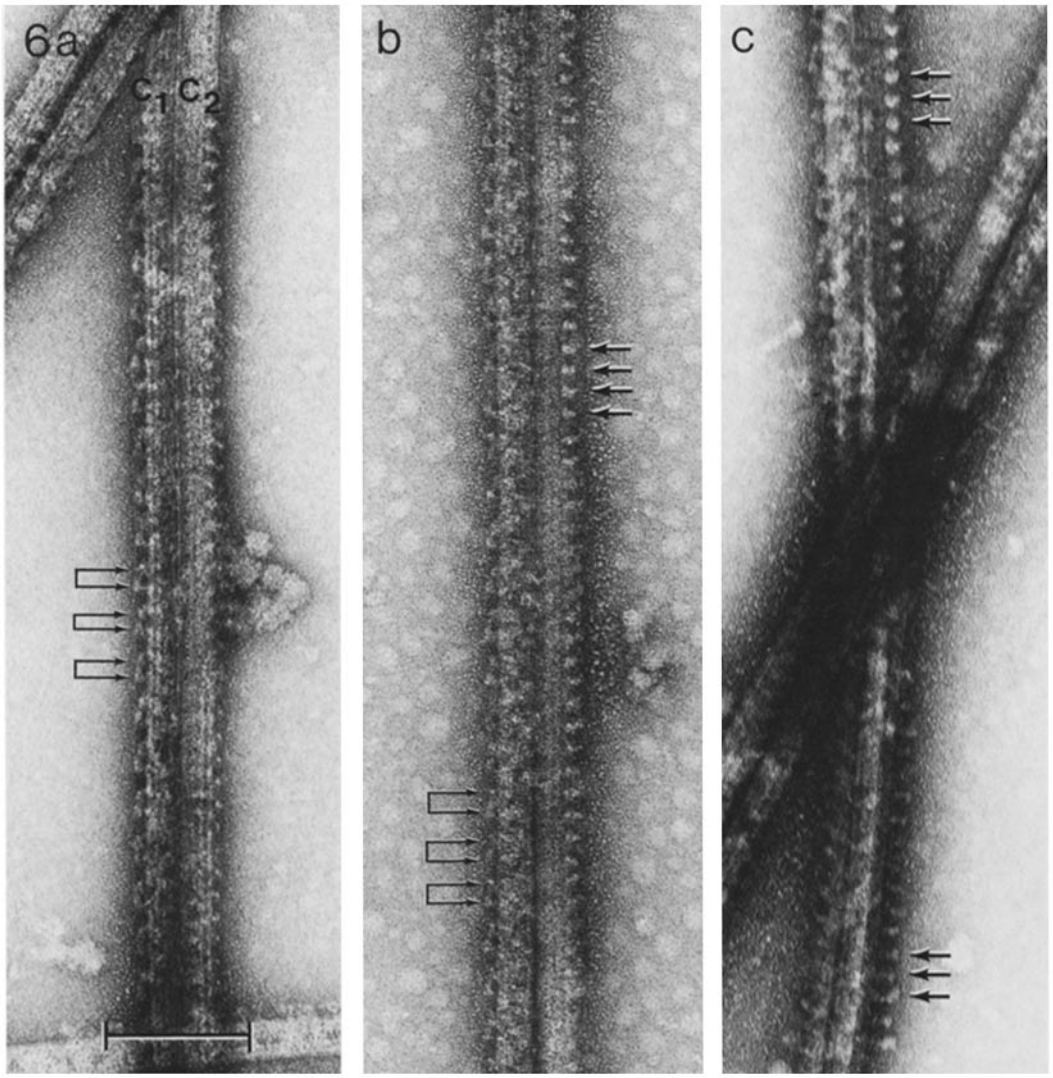

FIGURE 6 Isolated central-pair microtubule apparatus negatively stained. In each case the C_1 tubule is on the left. The C_1 tubule possesses a series of paired structures (double arrows) on its left-hand edge. The paired structures repeat axially with a 32-nm periodicity and a distance of 11 nm between members of a pair. It is not yet clear whether these paired structures form a single row of such components or are an artifact of superimposition of two rows of single globules out of phase by 11 nm (see Fig. 10). The tilting of the globular pairs indicates a polarity of the microtubule, although the absolute sense of polarity has not been determined here. The C_2 tubule has a single row of projections (single arrows) with an axial repeat of 16 nm. In *b*, these projections are oriented perpendicular to the page, appearing as large, electron-translucent dots. In *c*, the central pair twists in the plane of the carbon film; on the lower half of the tubule the projections appear in profile, being formed of a 5 × 15 nm shaft and an 8–9 nm diameter globular tip. Bar, 100 nm.

The C_1 Central Microtubule

The C_1 tubule in negative stain is characteristically mottled in appearance, whether it is associated with (Figs. 6 and 7) or free of its accessory structures (Fig. 8). The mottled pattern gives the impression of some regularly repeating material within the lumen of the microtubule; however, diffraction patterns of naked tubules reveal no organized structure other than the tubulin subunit lattice.

The C_1 tubule does not possess the 16 nm repeating projections; instead, structural elements repeating at 32 nm are attached along the outer edge of the microtubule (Fig. 6 *a* and *b*). In these longitudinal views of the intact central pair apparatus, two ellipse- or globe-shaped subunits (~7 × 9 nm) appear to be grouped into pairs (~11 nm between members of a pair); the axial repeat of such pairs is 32 nm center to center. Usually, one subunit of the pair is further from the tubule surface than the other, indicative of a polarity (or handedness) of the overall structure. In our previous study of rat sperm flagella (57), we suggested that each pair of closely spaced globular subunits formed a larger "barb-shaped" element that repeated axially at 32 nm. An equally likely explanation is that there are two staggered rows of globules, each with a 32-nm axial periodicity, and each arising from one of the columns of material seen in cross section attached to the outer lateral edge of the C_1 tubule (see Fig. 4 *c*, *d*, *e*, and Fig. 12). In this case, the apparent association of two globules into a dimer would arise as an artifact in a longitudinal view, due to the superimposition of the two staggered rows. The staggering and polarity of such globules would occur as a consequence of their binding to the underlying helical lattice of tubulin subunits and the tilt of the central pair about its axes in the electron microscope. Examples, such as those shown Fig. 10, show only a simple linear array of globules with an axial repeat of 32 nm; it is not clear,

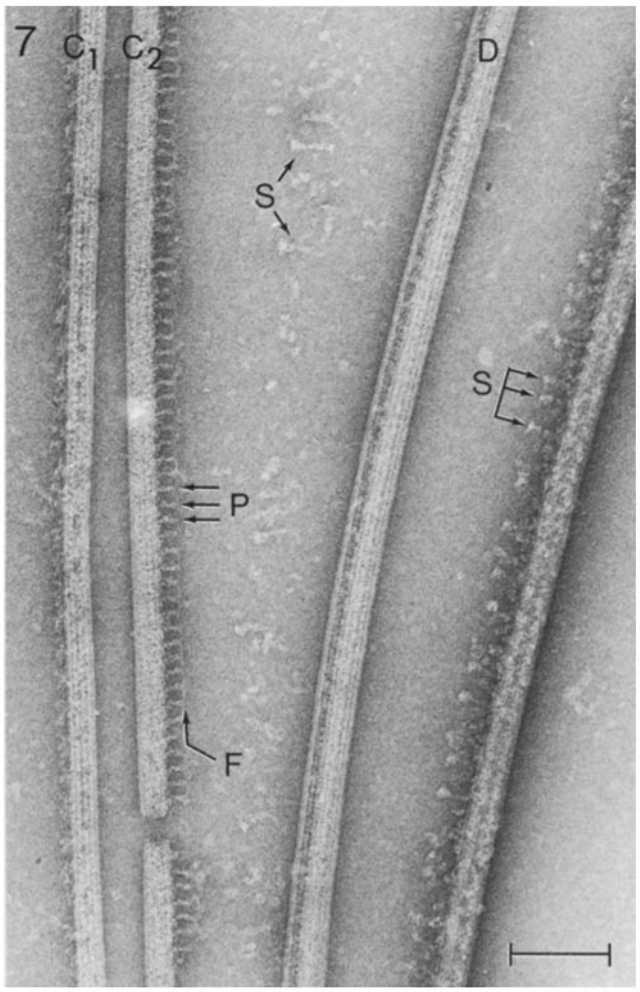

FIGURE 7 Elements of a demembranated squid sperm flagellum negatively stained. The C_1 tubule appears mottled, retaining some associated material along the left-hand edge. The C_2 tubule is stained more evenly, displaying a single row of 5 × 18 nm projections (*P*) with an axial repeat of 16 nm. The tips of the projections are connected by a filamentous strand (*F*). For comparison, a doublet microtubule (*D*) and radial spokes (*S*) are shown. The radial spokes measure 6 × 32 nm, and are seen both free and attached to a doublet tubule in their triplet arrangement. Bar, 100 nm.

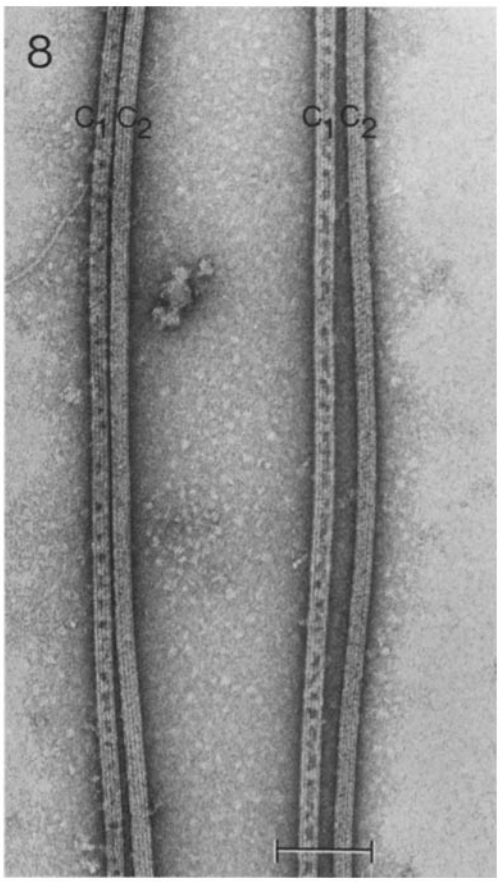

FIGURE 8 Isolated central-pair microtubules negatively stained. From this image and others (e.g., Fig. 7), it is clear that the two central microtubules are fundamentally different, even when all outer-surface-associated material has been fortuitously removed. The lumen of the C_1 tubule is unevenly filled with stain; the pattern is faintly periodic, although no definite structural repeat has been measured. The C_2 tubule is smooth and evenly contrasted by stain due to the apparent exclusion of stain from its lumen by the dense core of material seen in cross section (Figs. 3 and 4). Bar, 100 nm.

however, whether one of the two rows of globules has been extracted or, alternatively, whether the outer subunits have been lost from a single row of dimers.

The Basis of "Pairing"

The two members of the central-pair microtubules are joined at their closest points by what has been termed the "central bridge," which repeats at 16 nm axially (78).

In squid, the distance between the C_1 and C_2 tubules at their closest points is not more than 10 nm (Figs. 3 and 4). The bridging elements seen in Fig. 11*a* repeat at 16 nm axially. Two important details should be noted regarding this figure: first, the distance between the C_1 and C_2 tubules in this figure varies from 7 nm to 15 nm, yet the bridges accommodate the varying distance, remaining in contact with the two tubules. Second, these bridges contact the C_2 tubule in perfect register with the beaded chains described above; the bridges in fact appear to be continuous with the beaded chains and composed of the same linear arrangement of 7.5–10 nm diameter globular subunits. Thus, whether or not the central bridge is a separate structural entity is unclear; it seems most likely, from examples such as Fig. 11*a*, that the two central tubules are joined by contact between the C_1 tubule and the outer surfaces of the C_2 beaded chains. (We have so far been unable to determine whether the C_1 tubule also possesses such beaded-chain structures.) The apparent 15-nm-long bridges seen in Fig. 11*a* might thus have arisen from a partial unwinding of the beaded chains.

In solution, the isolated central microtubule apparatus frequently associate longitudinally (Fig. 12). This double pairing always occurs as a result of the association of the C_2 tubule of one central apparatus with the C_2 tubule of a second apparatus, thus forming a homologous (C_2-C_2') pair (Fig. 12*a*). We previously stated that this association occurs in an antiparallel (bipolar) fashion, basing our conclusion on the apparent polarities of the 32-nm repeating components of the C_1 and C_1' tubules (41). Further investigations on cross-sectioned material (Fig. 12*a*) show this conclusion was wrong; invariably, the two paired central apparatus are symmetrical about an axis between the two C_2 tubules, indicating that the two central-pair apparatuses are parallel (unipolar). (It has not been determined, however, whether the two microtubules within a native pair are parallel or antiparallel.)

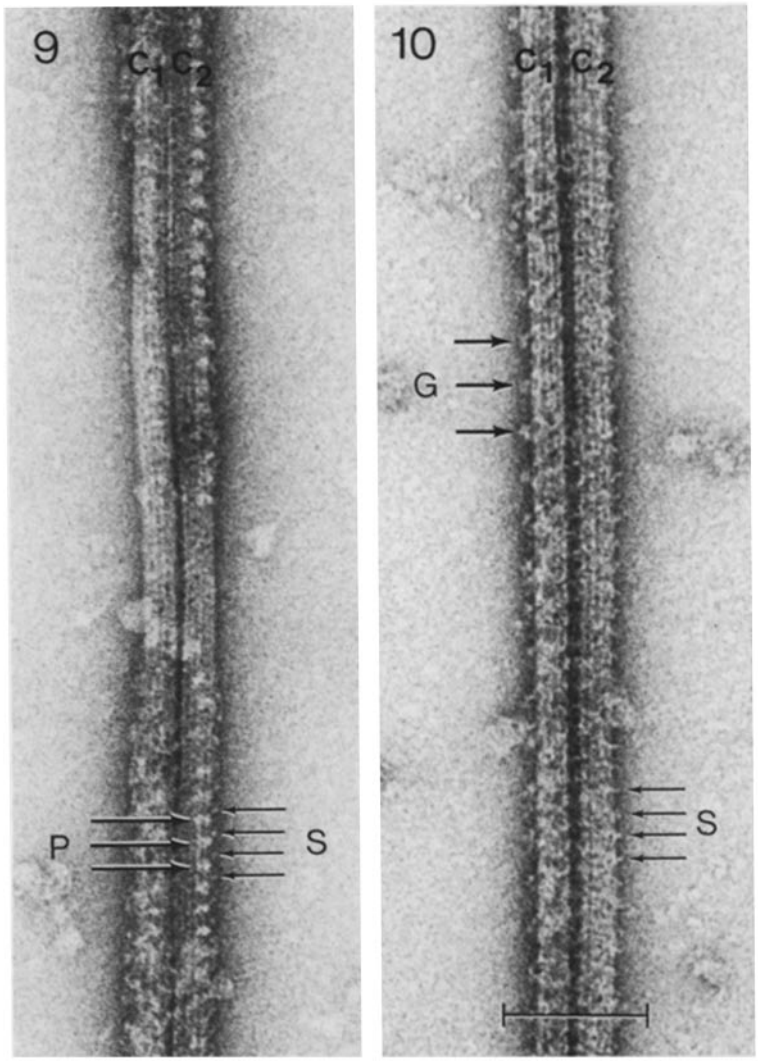

FIGURES 9 and 10 Isolated central pair microtubule apparatuses negatively stained. *9*: the projections (*P*) oriented perpendicular to the page appear as large, electron-translucent dots with an axial periodicity of 16 nm. A series of smaller structures (*S*) appear along the right hand edge of the C_2 tubule, also with a 16-nm periodicity, but out of register with the projections. The middle sections of the C_1 and C_2 tubules have been stripped of their associated surface structures, dramatically illustrating the thickness and complexity of the central sheath. *10*: small subunit structures (*S*) appear on the right-hand side of the C_2 tubule, as in Fig. 9; a faint indication of this material, possibly wrapping around the tubule and passing through the intertubule space can be seen. Large 7- to 9-nm globules (*G*) are arranged along the left-hand edge of the C_1 tubule with an axial spacing of 32 nm. These globular structures probably correspond to a single row of such elements seen in cross section (Fig. 4 *c* and *d*). Bar, 100 nm for Figs. 9 and 10.

The phenomenon of the homologous C_2-C_2' pairing is interesting and may explain the native heterologous C_1-C_2 pairing. In negative stain preparations (Fig. 12*b*), in the region between the two C_2 tubules, a series of electron-transparent dots (i.e., protein) are seen with an axial repeat of 16 nm; further analysis (data not shown) has confirmed that these dots arise from the beaded chains around the C_2 tubules. Thus, we propose that the in vitro homologous pairing, as well as the in vivo heterologous pairing, is a direct result of the interactions between the C_2 beaded chains and the adjacent microtubule, be it a C_1 tubule or another C_2 tubule. Depending on their mode of interaction, the beaded chains of the C_2 and C_2' tubules may be in or out of phase, resulting in a single or double set of bright dots in negative stain in the intertubule space. The fact that only a single set of dots is seen repeating at 16 nm axially (Fig. 12*b*) suggests that the beaded chains of the C_2 tubule are in register, possibly interlocking, with those of the C_2' tubule.

DISCUSSION

Nomenclature for the Central Sheath and Central-Pair Microtubules

The term "central sheath" was originally used to refer to the regularly spaced striations that appeared to wind helically around the two central tubules (28). Subsequently, it was shown that the central tubules possess rows of projections that repeat axially with a periodicity of 16 nm (14, 30, 59, 76, 79). Because separate filaments have never actually been observed helically wrapped about the central pair apparatus, it was suggested that it is the projections that form the central sheath (14, 59); thus, these structures have been termed the "central sheath projections" (78, 79). We feel that the term "central sheath" should include all microtubule-associated structures of the central pair, i.e., the 16 nm-repeating sheath projections, the 32-nm-repeat-

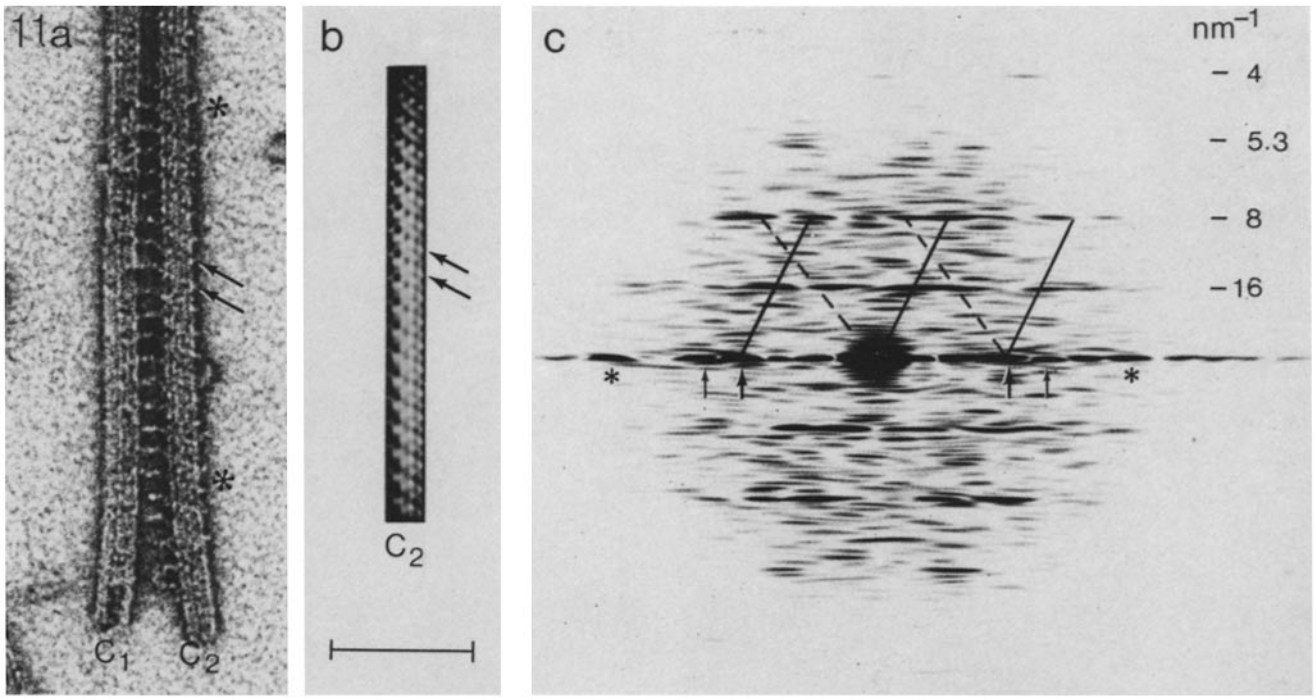

FIGURE 11 Optical diffraction/reconstruction analysis of the C_2 microtubule imaged by negative-stain electron microscopy. *a:* Negative-stain image of central-pair microtubules isolated from squid sperm flagella, showing the C_1 and C_2 tubules linked by the so-called central bridges that appear as rungs with an axial repeat of 16 nm. The space between the C_1 and C_2 tubules (and the length of the bridges) varies from 7 nm (up and out of the field of view) to 15 nm (lower). The bridging elements appear to be composed of 7-nm globular subunits and are in register with the helix-like striations (arrows) associated with the C_2 tubule. Positive identification of the C_1 and C_2 tubules was made on the basis of their associated sheath components, out of the field of view. *b:* Filtered image (optical reconstruction) based only on the reflections on the lattice of the near side (*c*). It shows a helix-like arrangement of 10-nm globular subunits, arranged around the C_2 microtubule in the manner of a beaded chain or necklace. *a* and *b* are arbitrarily shown with a left-handed beaded chain. Bar in *a* and *b*, 100 nm. *c:* Optical transform of the C_2 tubule masked to include the area between the asterisks in *a* and exclude the horizontal bridging elements. The exact steric relationship of the transform to the specimen has been maintained during the photographic manipulations. The transform shows off-meridional reflections on the 4, 5.3, 8, and 16 nm^{-1} layer lines, and equatorial reflections at 5 nm^{-1} (asterisk), 7.5 nm^{-1} (small arrows), and 10 nm^{-1} (large arrows). Together with the off-meridional reflections, the 7.5–10 nm^{-1} equatorial reflections show the presence of a helix-like arrangement of globular, not fibrous, components. The characteristic reflections from the J_3 and J_{10} Bessel orders of the tubulin monomer subunit lattice (6) are seen on the 4-nm^{-1} layer lines. The inked lines show the tentative indexing of the diffraction pattern: arbitrarily, the solid lines represent the near side and the dashed lines the far side of the specimen. The 10-nm^{-1} equatorial reflections and the 8- and 16-nm^{-1} off-meridional reflections fall almost exactly on the intersections of the layer lines and the solid, inked indexing lines. Two unit cells of 10 × 16 nm^{-1} are shown for the near side, although a third is clearly present in the left half of the transform. The helix-like arrangement of the 10- × 16-nm unit cell, i.e., the beaded chain, appears to extend to the J_3 and J_{10} reflections on the 4-nm^{-1} layer line and to superimpose on the helically symmetric lattice of the A tubule as proposed by Amos and Klug (6); this relationship may only be a coincidence, arising from the radius of mass distribution of the beaded chain being greater (~18 nm) than that of tubulin (~11 nm).

ing globular sheath components, and the 16-nm-repeating beaded chain. The appearance in Fig. 9 of the central-pair microtubules actually ensheathed by associated protein structures verifies the appropriateness of the term.

The two microtubules comprising the central-pair apparatus were described earlier by their positions within the axoneme rather than by any morphological criteria (79); i.e., the C_3 and C_8 microtubules were defined by their proximity to outer doublet microtubules 3 and 8, respectively. Recently, a report has appeared that provides evidence that the central pair of *Paramecium* cilia may rotate as a unit within a nine-fold cylinder of outer doublet microtubules (58); if this is true, reference to the C_3 and C_8 tubules becomes meaningless in the absence of a 5–6 bridge. Although the rotation of the central pair may not be a mechanism general to all cilia and flagella, it would nevertheless be desirable to define the central-pair nomenclature unambiguously.

The two central tubules have been shown to differ markedly in their stability with respect to chemical extraction; this distinction has been observed in *Chlamydomonas* flagella (32), scallop gill cilia, and sperm flagella (37, 38), and sea urchin sperm flagella (21). The two individual central tubules have also been shown to differ morphologically. In *Tetrahymena* cilia (3, 14), one of the central tubules possesses one row of 18-nm-long projections with an axial repeat of 16 nm; this same tubule also possesses a second row of shorter structures whose axial periodicity is less certain, but is reported to be 16 nm. The second central tubule of *Tetrahymena* cilia was not seen to have any 16 nm-repeating structures. In a later study of *Tetrahymena* cilia, Chasey (16) demonstrated that only one of the tubules, the C_1 tubule, possessed a prominent 32-nm axial spacing, as observed in optical transforms of negatively stained material. Chasey's 32-nm repeat was apparently erroneously attributed to a perturbation in the 16 nm-repeating projection, because Olson and Linck (56) showed that in rat sperm the 32-nm repeat arises from the linear attachment of the globular

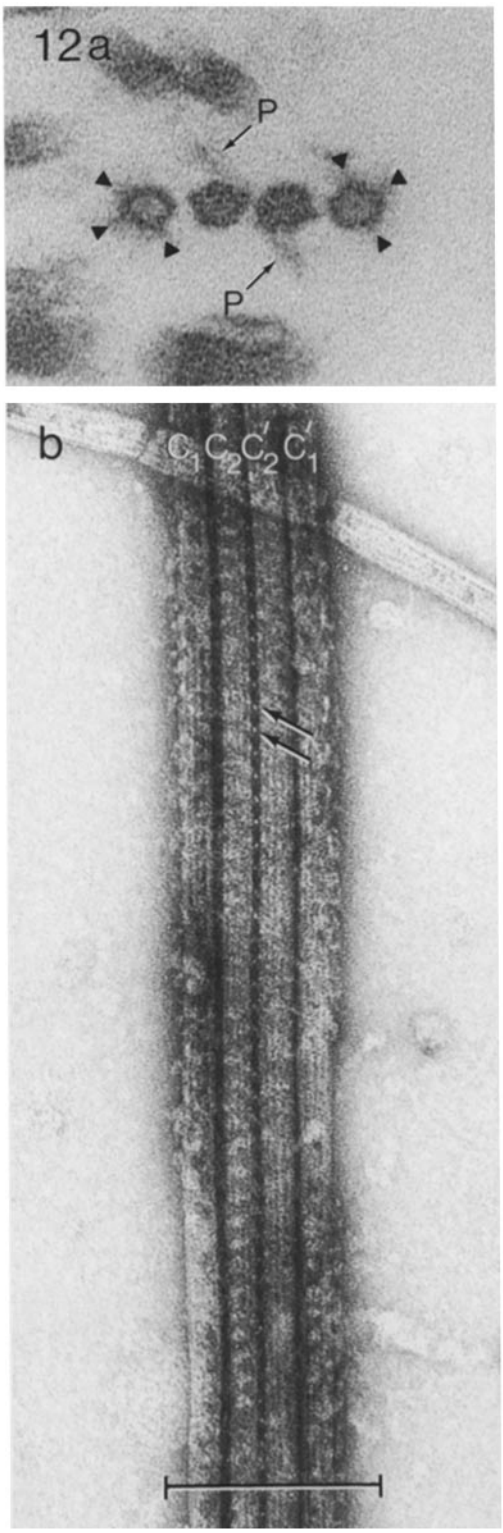

FIGURE 12 Isolated central-pair apparatus frequently form paracrystals as shown here. Thin-section and negative-stain analyses indicate that this double pairing is always accomplished by the association of the two C_2 tubules in a unipolar or parallel fashion, so that the two central pairs (C_1-C_2 and C_1'-C_2') have two-fold rotational symmetry about an axis between the two C_2 tubules. In thin section (*a*), the C_1 tubules (hollow) and the C_2 tubules (possessing a dense granular core) can be distinguished; the C_1 globular sheath components (▲) and the C_2 projections (*P*) can be readily seen (cf. Figs. 3 and 4). In negative stain (*b*), the C_1 and C_2 tubules are distinguished (cf. Figs. 6 and 7). The most important feature here is a series of bright dots (arrows) in between the C_2 and C_2' tubules. The space measures 7–10 nm wide. The dots are arranged with an axial repeat of 16 nm. Helix-like striations can be seen on the C_2 tubules along the arrow axis. It is likely that the bright dots originate from the same protein structures apparent on the right-hand free edge of the C_2 tubules of Figs. 9, 10, and 11, and that it is these same 7.5- to 10-nm globular subunits that form the beaded chains (Fig. 11).

sheath components, not the 18-nm-long sheath projections. In this and our earlier paper (56), we have adopted the convention that the C_1 tubule possesses the 32-nm repeating globular sheath components. Such a convention seems to hold for squid and rat sperm, as we have never observed a 32-nm repeat associated with the C_2 tubule. However, we cannot say from negative stain EM analysis alone whether the C_2 tubule in these and other species cannot also possess similar or different 32-nm repeating structures.

A second criterion also provides an independent means of identifying the central tubules in some species. An electron-dense granule or fiber is observed in cross sections of cilia and flagella of some species (ctenophores [31, 73] and molluscan gill cilia [2, 24]). Our evidence indicates that this structure is a fixation artifact arising from a single row of sheath projections (data not shown). Thus, the central tubules can be numbered as follows and as shown in Figs. 3 and 4: with the axoneme viewed in its clockwise enantiomorphic form (dynein arms clockwise), and with the single projection or dense granule thereof oriented up, the C_1 tubule then appears on the left and the C_2 tubule on the right.

Structure of the Microtubule

Microtubules have been assumed by most investigators to be helically symmetrical. Amos and Klug (5, 6) investigated the tubulin dimer lattices of flagellar doublet microtubules by Fourier analysis of EM images of negatively stained material. Their results indicated that the tubulin dimer lattices of the A and B tubules are different. Because the A tubule is a cylindrical, 13-protofilament microtubule, and because the B tubule is an incomplete cylinder composed of 10–11 profilaments (75), it was generally assumed that the symmetrical lattice of the A tubule, or the A lattice, was the correct one for all singlet microtubules. Earlier, Chasey (15) had concluded from diffraction analysis of negatively stained central-pair microtubules that the dimer lattice was staggered and symmetrical (as suggested for the A tubule). On the other hand, the x-ray studies by Mandelkow and colleagues (47, 48) of reassembled brain microtubules could not resolve 8-nm layer-line reflections, although these workers noted that the x-ray patterns were not consistent with the A lattice. Similarly, McEwen and Edelstein (50) have shown evidence that reassembled brain microtubules possess a mixed lattice (both A and B lattices, but principally the B lattice) and thus helical discontinuities. Of course, the difficulty in studying synthetic microtubules is that microtubules may not reassemble in vitro with the correct, native arrangement of tubulin dimers, whereas the diffraction studies of native microtubules may not reveal chemical asymmetries. In fact, Linck (39), Meza et al. (52), and Witman et al. (80, 81) have shown that flagellar A tubules are not chemically symmetrical because one or more three-protofilament segments (ribbons) were resistant to solubilization. Linck showed further that specific nontubulin proteins were associated with the resistant three-protofilament ribbons and suggested that the

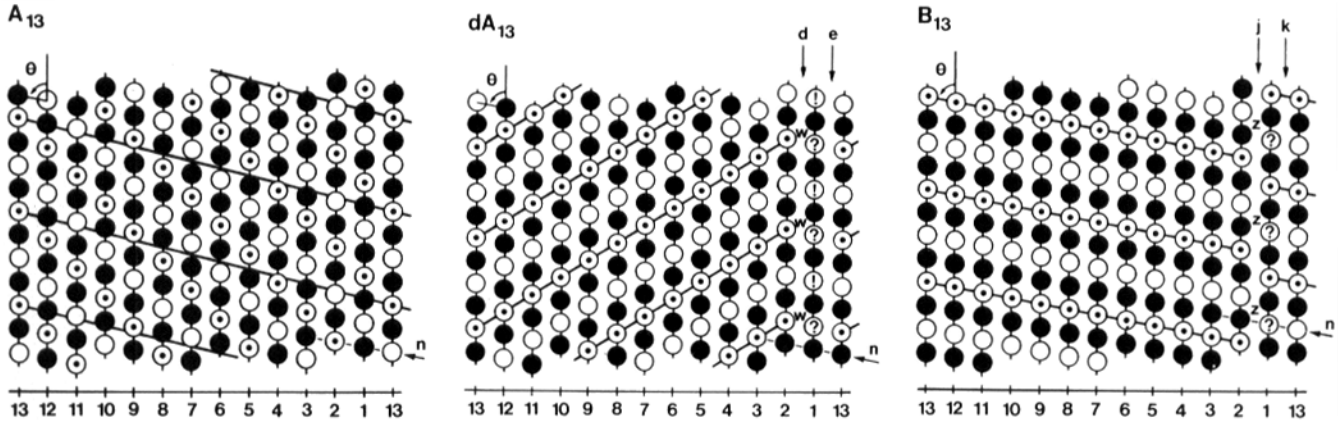

FIGURE 13 Subunit lattices in the C_2 central-pair microtubule: the longitudinal (vertical) protofilaments are composed of alternating α (open circles) and β tubulin (filled circles), believed to form the polar-directed $\alpha\beta$-tubulin heterodimer (6, 46). All models possess a left-handed, 3-start helical family (*n* arrow) that, with the protofilaments, defines the monomer lattices and an ~4-nm axial × 5-nm equatorial unit cell (6, 19, 42, 50). θ is the smaller bond angle of the tubulin monomer unit cell. The model design permits one to photocopy and roll them into cylinders by superimposing the repeated 13th protofilaments. Open circles with dots designate a unique population of α_2 tubulin subunits. Evidence indicates that microtubules are composed of equimolar ratios of two α-tubulins and/or two β-tubulins (9, 10, 45, 70, 71). For simplicity, we illustrate only the different α_1 (open circles) and α_2 subunits (circles showing . ? !). Model A_{13} assumes the helically symmetric lattice of tubulin dimers, as proposed by Amos and Klug (6) and Bibring et al. (10) for flagellar A tubules. The beaded-chain locus is shown as a 1-start, left-handed helix with a 16-nm pitch (diagonal line); this locus is arbitrarily chosen, given the limited possibilities of the chain being left- or right-handed and approximately 1- or 2-start. The lattice of the chain does not coincide with that of the microtubule, nor do the other possible loci of the chain. If the beaded chain is to interact regularly with the microtubule surface lattice, the latter must be helically asymmetric, given the structural parameters of the chain.[1] Two more likely microtubule models are presented below. Although possibly incomplete or incorrect in details, these models show the concepts important to singlet and double microtubule structure. The models leave open the possibility that the subunits of the beaded chain interact with individual protofilaments or with pairs of protofilaments. Do not assume in these models that all protofilaments are composed solely of tubulin. Model dA_{13} assumes the A lattice of dimers, but protofilament 1 (and possibly 2) is either chemically unique and/or assembles as shown in a phase-shifted manner, producing a helical dislocation in the dimer lattice. The beaded chain (diagonal bars) can be arranged on identical tubulin lattice points as shown. The lattices of the microtubule and the beaded chain are asymmetric, with the latter taking the form of dislocated helices (beaded lock washers) with a 16-nm axial repeat and a pitch of ~34 nm (a right-handed and nearly 2-start helix). Model B_{13} assumes the tubulin dimer lattice of the incomplete B tubule. This model automatically creates a helical discontinuity between protofilaments 1 and 2. The beaded chain can be arranged on identical lattice points as shown. Again, the microtubule and beaded chain are asymmetric, with the latter taking the form of lock washers with a 16-nm axial repeat and a pitch of ~12 nm (a left-handed and nearly 1-start helix). Consequences of the models: first, models dA_{13} and B_{13} possess one or two helical dislocations (seams) *d*, *e*, *j*, and *k*, depending on where α_2 tubulin assembles in protofilament 1 (. ? !). The two seams within one microtubule may or may not be sterically identical. If in protofilament 1 of B_{13}, α_2 = ., then B_{13} possesses only a j seam; whereas if α_2 = ?, the B_{13} possesses j and k seams that are sterically different. dA_{13} has more complicated seam sets, depending on the assumptions regarding the assembly of α_2-tubulin. The seams and/or unique chemical nature of the relevant protofilaments may lead to the stable ribbons observed in Fig. 2 of Linck and Langevin (44). Second, models dA_{13} and B_{13} also have stereospecific sites (e.g., w and z sites) that repeat axially at 16 nm and could specify the spatial distribution of various microtubule-associated components, e.g., the C_2 sheath projections.

ribbon protofilaments themselves were composed of chemically unique tubulins or tubulinlike proteins (39). Clearly, then, a further investigation of stable, singlet microtubules such as the central-pair microtubules of flagella would be valuable.

Our findings on the central-pair apparatus of squid sperm flagella have not yet defined the lattice of tubulin dimers in these microtubules, but they do suggest that these microtubules are not helically symmetric with respect to the dimer lattice. This conclusion rests partly on our investigation of the beaded-chain structure associated with the outer surface of the C_2 central tubule. This structure's axial periodicity is 16 nm, and the pitch approximates a one-start or two-start (upper limit) helix, i.e., the helical pitch is close to either 16 or 32 nm. If we assume for a moment that the beaded chain is arranged on a perfect 16-nm, one-start helix, and that the surface lattice of the C_2 central tubule is that of the A tubule, it is evident from Fig. 13*A*$_{13}$ that the 16-nm helix does not fit into the lattice of the microtubule. The same is true whether the beaded chain is one- or two-start or right- or left-handed. It is doubtful that quasi-equivalent bonding (13) could explain the drastically different protein-protein interactions required for a structure such as illustrated in Fig. 13*A*$_{13}$, inasmuch as the chain is apparently not fibrous but composed of discontinuous globular subunits (Fig. 11).

The association of the beaded chain with the microtubule can better be explained by either of two simple models: the reader is now referred to Fig. 13: *dA*$_{13}$ and *B*$_{13}$. Identical models were independently deduced in the accompanying study (44). At present, we do not have sufficient information to distinguish between the models *dA*$_{13}$ or *B*$_{13}$, nor do we know whether the structures of both the C_1 and C_2 central microtubules are identical. Different types of microtubules may in fact have

[1] The tubulin lattice could be symmetrical if the chain were self-terminating after one turn; however, current results indicate that microtubules are chemically asymmetric with respect to the protein composition of the protofilaments (R. Linck, D. Albertini, G. Langevin, G. Olson, and D. Woodrum. 1981. *Biophys. J.* 33:215*a*).

different lattice structures.

Although these models are still tentative, the basic premise that the C_2 central microtubule is structurally (and possibly chemically) asymmetric begins to explain several features of microtubules. First, the underlying complexity of the tubulin subunits themselves may provide the basis for the axial and circumferential arrangement of microtubule-associated structures such as the beaded chain. Second, the presence of the stereospecific sites between certain pairs of protofilaments may govern the axial (i.e., linear) distribution of associated components along the microtubule. For example, the binding of the single row of sheath projections and its 16-nm axial repeat could be specified by such a model. Finally, the unique seams between certain protofilaments may confer a greater stability to one portion of the microtubule wall, e.g., a ribbon of 2–5 protofilaments, depending on the number and type of seams present and the potential influence of associated ribbon-specific proteins (39). Although we did not attempt to chemically fractionate squid central pair microtubules, the results described in the accompanying paper clearly indicate that the central-pair microtubules of sea urchin sperm possess at least one such stable ribbon per microtubule (see Fig. 2 of Linck and Langevin [44]).[2] Similar excellent examples appear without comment in Figs. 1 and 3 of Meza et al. (52). Furthermore, the presence of helical dislocations in the form of seams between certain protofilaments in the wall of microtubules provides a molecular basis for the stable ribbons of two and three protofilaments isolated from flagellar A tubules (23, 39, 40, 43, 52, 77, 80, 81), and may also be important in explaining the assembly of brain tubulin into ribbons of 3–5 protofilaments in vitro (48, 49, 63). We suggest that such ribbons may be important to the structure and function of all cytoplasmic microtubules.

Pairing—the Central Bridge

The two microtubules of the central pair are seen in cross section to be joined by a structure termed by Warner (78) the "central bridge." The nature of this bridge is not so readily apparent in longitudinal view; however, Warner (78) has shown the best images to date of this structure in mussel gill cilia and established its axial periodicity as ~16 nm. In our investigations we find: (*a*) that the gap between the C_1 and C_2 tubules is not >10 nm in fixed-embedded or in negatively stained material (in agreement with Warner); (*b*) that the central bridges are in perfect register with the beaded chains of the C_2 tubule (Fig. 11); and (*c*) that the bridging elements appear to be composed of similar 7.5- to 10-nm globules that form the beaded chain (Fig. 11). This evidence suggests the pairing of the C_1 and C_2 tubules results from an association between the outer surface of the C_2 beaded chains and the surface of the C_1 tubule. We do not know yet whether the C_1 tubule also has such beaded chains; if so, this might explain the suggestion that in some species the central bridge is composed of two parallel subunits (24, 78, 82). Credence is given to our model by the facts that pairing is observed to occur in vitro between homologous C_2 tubules of different central pair apparatuses (Fig. 12) and that the axial repeat and bonding distances of the bridging elements (i.e., beaded chains) are the same between homologous pairs (Fig. 12) as between native heterologous pairs of tubules (Figs. 4, 9–11).

The 16-nm-repeating Sheath Projections

There is a single row of sheath projections associated with the C_2 tubule of squid central pair. The molecular mechanism by which only a single row of structures attaches to the microtubule surface lattice with a 16-nm repeat was discussed above. Other organisms also appear to have only a single row of 18-nm-long sheath projections. In cross sections of *Tetrahymena* cilia, Allen (3) noted such a projection attached to one of the two central tubules, and in *Paramecium* cilia Omoto and Kung (58) described a similar "spur" attached to one of the tubules. For *Tetrahymena*, Chasey (14) demonstrated the axial spacing of this set of long projections to be 16 nm. The axial spacing of this component was not determined in *Paramecium* (58), but it is clearly arranged in an axial fashion along the microtubule, and it seems likely from the position of the "spur" that it corresponds to the single sheath projection in squid sperm. On the basis of our criteria discussed above, we conclude that also in these other species the single prominent row of sheath projections binds to the C_2 tubule.

Although the central pair of squid have but a single row of 18-nm-long projections (i.e., associated with the C_2 tubule), other species differ in this regard; however, conclusions from interspecies comparisons are difficult to make from the existing literature due to the lack of resolution in thin-section analysis, the potential lack of structural preservation in negative stain, and the subjective interpretations of the investigators. Nevertheless, the central pair clearly has a more complex structure in fresh-water mussel gill cilia (79), rat sperm flagella (56), and *Chlamydomonas* flagella (82). In these cases, both central tubules appear to possess two rows of structures resembling projections. Unfortunately, the strucutral and chemical identity of these multiple rows of sheath components has not been established. There may, in fact, be several different types of 16-nm-repeating projections. In the examples of *Chlamydomonas* shown by Hopkins (30), the β-projections of his Fig. 15 clearly resemble the 18-nm-long projections of squid, whereas the α-projections in this figure do not. Possibly, the α-row represents a set of shorter projections, or may even be an artifact produced by the unwinding of the beaded chains.

The 32-nm-repeating Sheath Components

In the squid central pair, the 16-nm-repeating projections have never been seen, in negative stain, to be associated with the C_1 tubule; instead, structures of a globular nature are seen arranged with a 32-nm axial periodicity. Conversely, the 32-nm-repeating sheath components have so far not been resolved on the C_2 microtubule. Because, presumably, three separate rows of globular components are attached to the surface of the C_1 tubule in cross section (Fig. 4), it is not clear whether the paired appearance of the globules in longitudinal view (Fig. 6 *a* and *b*) is characteristic for each of these rows or whether it arises from the superimposition of the two outer rows. The chemical identity of these three rows of sheath components is also unknown.

These 32-nm-repeating globular sheath components are not unique to squid sperm. We originally discovered these structures attached to only one of the central tubules in rat sperm (56) and have observed them in association with one of the central tubules of sea urchin and scallop sperm and scallop gill cilia (unpublished observations). Also, in published micrographs of fresh-water gill cilia (Fig. 11 *a* and *b* of Warner and Satir [79]), we have detected the appearance of a 32-nm glob-

[2] We thank Dr. I. R. Gibbons for helpful discussion on this matter.

ular repeat associated with one of the central tubules. Chasey (16) originally demonstrated by optical diffraction analysis that a 32-nm axial repeat was present in only one of the two central pair microtubules; the 32-nm repeat, however, was ascribed to a perturbation of the central sheath projections by the radial spokes, rather than to an inherent structural component of the central tubule. Finally, Witman et al. (82) described some of the details of the central sheath components of *Chlamydomonas* flagella in mutants lacking the radial spokes, noting in cross sections that, whereas one of the central tubules possesses two long projections (in agreement with Hopkins [30]), the other tubule has two shorter structures, although no information was provided as to the longitudinal arrangement of such components. Hopkins (30) reported that the axial periodicity of one of these shorter structures was about 16 nm; however, it is possible that he was viewing the superimpositions of two half-staggered rows of 32-nm-repeating globular sheath components and, thus, only an apparent 16-nm periodicity. In our opinion, Hopkin's Fig. 16 supports such a conclusion, and 32-nm periodic structures along microtubules can be seen clearly in some of his micrographs.

Components Associated with the Microtubule Lumen

The C_1 and C_2 tubules of squid sperm flagellar central pair was strikingly different, even after the surface-associated material has been stripped away (Fig. 8). Their appearances in negative stain and in cross section appear to be correlated as follows: the C_2 tubule in negative stain (Figs. 6–8) appears smoother and more evently stained because its lumen (in cross section, Fig. 4) is entirely filled with extra material that apparently occludes uranyl acetate; thus, the tubule is contrasted only on its outer, smooth surface. The C_1 tubule, on the other hand, appears mottled in negative stain (Figs. 6–8) because, presumably, extra material is periodically arranged along the lumen, permitting uranyl acetate to accumulate inside. No organization of the lumen-associated material has yet been found by optical diffraction analysis. It may be that in the C_2 tubule the lumenal material is not contrasted by negative stain, or that in the C_1 tubule the organization of the lumenal material is disrupted by the low pH of uranyl acetate.

Several investigators have noted the presence of extra material within in the lumens of the ciliary and flagellar microtubules (11, 17, 24, 38, 39, 44, 60, 66, 80). The functions of these potentially lumen-associated proteins are unknown. Perhaps they play a role in microtubule assembly or confer special mechanical properties to the assembled microtubules, or perhaps they are enzymes required for flagellar function. From the work of Farrel and Wilson (21), Jacobs et al. (32, 33), and Linck (37, 38), we know that one of the two central tubules is more resistant to solubilization than the other; perhaps lumen-associated proteins are responsible for the stability of these and other cytoplasmic microtubules.

Functional Importance of the Central Pair: Regulation of Motility

In the cilia and flagella of some species, the central region of the axoneme is occupied not by a central pair of microtubules but by one or more than two microtubules, or by a nonmicrotubular axial core (17, 29, 60). In yet other species, the central region of the axoneme is apparently devoid of any central structure (17, 60, 61). In all of these cases, the different species of cilia and flagella are fully motile. Although the central pair is not essential for motility in some species, flagella of species (e.g., *Chlamydomonas*) that naturally possess a central pair can become paralyzed if it is genetically deleted (82). Some studies have shown that flagella that possess an axial core (60) or that are completely devoid of any central structure (61) beat in a helical manner, instead of in the essentially planar wave characteristic of many 9 + 2 flagella. The important point here is not whether the central pair is essential for ciliary and flagellar motility, but probably that the central-pair apparatus (or its equivalent) is a species-specific adaptation for the regulation of motility, e.g., for the appropriate ciliary or flagellar wave form. Perhaps, it is also important for chemotaxis, phototaxis, and directionality of beat.

The direction of ciliary and flagellar bending has been shown to bear a relationship to the coaxial plane of the central tubules (22, 24, 26, 74), although it has not been established whether this is a causal relationship. Warner and Satir (79) demonstrated that ciliary bending was accompanied by sliding between the radial spokes and the central-pair microtubule apparatus and proposed that cyclic spoke–central pair cross-bridges might act to convert outer doublet sliding (64, 65, 72) into bending waves. These results were later supported by the work of Witman et al. (82). However, it has now been shown that small groups of doublet tubules—free of the central pair—will themselves generate bending waves (55); thus, the exact mechanism by which the central pair regulates motility may not be so straightforward as originally proposed.

Two further sets of investigations shed light on how the central pair might regulate motility. First, evidence has been presented showing that the central pair of *Opalina* (74) and *Paramecium* (58) cilia twist or rotate within the cylinder of the outer nine doublet microtubules. Such a rotation appears to occur in *Paramecium* with a frequency of one revolution per ciliary beat. These authors (58) propose that phase alignment of the rotating central pair with the outer doublets is what signals and coordinates the sliding movements of the latter to produce a three-dimensional wave characteristic of a cilium. The work of Tamm,[3] however, indicates that the rotation of the central pair may not be a general phenomenon, because the central pair does not rotate in metazoan cilia and suggests further possibilities for their role in motility.

Finally, Linck and colleagues (56, 62) have shown that rat sperm can be demembranated so that only doublet tubules 4–7 will actively slide in sequence in the presence of ATP, and that the sliding activity of doublet tubule 4 can be switched off by a subtle pH shift in the medium. Although more complicated explanations could be invoked, these results support the hypothesis that different doublet tubules may be activated or prevented from sliding by means of a signal-transduction mechanism involving the radial spokes and the central-pair microtubule apparatus.

The molecular mechanisms by which the central pair regulate ciliary and flagellar motility are not yet understood. The answers will ultimately come from our understanding of the structural and biochemical functions of the various microtubule-associated components discussed in this paper.

We are grateful to Andrea Golden for her assistance with the preparation of the manuscript and, in particular, the construction of Fig. 13, and to Drs. D. Albertini and D. T. Woodrum for stimulating discussion and reading of the manuscript.

[3] S. L. Tamm. Personal communication.

This work was supported by research grant GM 21527 from the National Institutes of Health and a Steps Toward Independence Award from the Marine Biological Laboratory to R. W. Linck, and by research grant HD 11816 from the National Institues of Health to G. E. Olson.

Received for publication 14 August 1980, and in revised form 18 November 1980.

REFERENCES

1. Afzelius, B. 1959. Electron microscopy of the sperm tail. Results obtained with a new fixative. *J. Biophys. Biochem. Cytol.* 5:269–278.
2. Afzelius, B. 1961. The fine structure of the cilia from ctenophore swimming-plates. *J. Biophys. Biochem. Cytol.* 9:383–394.
3. Allen, R. D. 1968. A reinvestigation of cross sections of cilia. *J. Cell Biol.* 37:825–831.
4. Amos, L. A. 1977. Arrangement of high molecular weight associated proteins on purified mammalian brain microtubules. *J. Cell Biol.* 72:642–654.
5. Amos, L. A. 1979. Structure of microtubules. *In* Microtubules. K. Roberts and J. S. Hyams, editors. Academic Press, Inc., New York. 1–64.
6. Amos, L. A., and A. Klug. 1974. Arrangement of subunits in flagellar microtubules. *J. Cell Sci.* 14:523–549.
7. Anderson, W. A., and P. Personne. 1967. The fine structure of the neck region of the spermatozoa of *Helix aspersa*. *J. Microsc. (Paris)* 6:1033–1042.
8. Baccetti, B., B. Pallini, and A. G. Burrini. 1976. The accessory fibers of the sperm tail. III. High-sulfur and low-sulfur components in mammals and cephalopods. *J. Ultrastruct. Res.* 57:289–308.
9. Berkowitz, S. A., J. Katagiri, H. K. Binder, and R. C. Williams, Jr. 1977. Separation and characterization of microtubule proteins from calf brain. *Biochemistry* 16:5610–5617.
10. Bibring, T., J. Baxandall, S. Denslow, and B. Walker. 1976. Heterogeneity of the alpha subunit of tubulin and the variability within a single organism. *J. Cell Biol.* 69:301–312.
11. Binder, L. I., and J. L. Rosenbaum. 1978. In vitro assembly of flagellar outer doublet tubulin. *J. Cell Biol.* 79:500–515.
12. Bryan, J. 1974. Biochemical properties of microtubules. *Fed. Proc.* 33:152–157.
13. Caspar, D. L. D., and A. Klug. 1962. Physical principles in the construction of regular viruses. *Cold Spring Harbor Symp. Quant. Biol.* 27:1–24.
14. Chasey, D. 1969. Observations on the central pair microtubules from the cilia of *Tetrahymena pyriformis*. *J. Cell Sci.* 5:453–458.
15. Chasey, D. 1972. Subunit arrangement in ciliary microtubules from *Tetrahymena pyriformis*. *Exp. Cell Res.* 74:140–146.
16. Chasey, D. 1972. Further observations on the ultrastructure of cilia from *Tetrahymena pyriformis*. *Exp. Cell Res.* 74:471–479.
17. Dallai, R. 1979. An overview of atypical spermatozoa in insects. *In* The Spermatozoon. D. W. Fawcett and J. M. Bedford, editors. Urban and Schwarzenberg, Baltimore. 253–265.
18. Drew, G. A. 1919. Sexual activities of the squid *Loligo pealei* (Les.). II. The spermatophore: its structure, ejaculation, and formation. *J. Morphol.* 32:379–435.
19. Erickson, H. P. 1974. Microtubule surface lattice and subunit structure and observations on reassembly. *J. Cell Biol.* 60:153–167.
20. Fairbanks, G., G. F. Steck, and D. F. H. Wallach. 1971. Electrophoretic analysis of the major polypeptides of the human erythrocyte membrane. *Biochemistry* 10:2606–2617.
21. Farrell, K. W., and L. Wilson. 1978. Microtubule reassembly *in vitro* of *Strongylocentrotus purpuratus* sperm tail outer doublet tubulin. *J. Mol. Biol.* 121:393–410.
22. Fawcett, D. W., and K. R. Porter. 1954. A study of the fine structure of ciliated epithelia. *J. Morphol.* 94:221–281.
23. Gattass, C. R., and G. B. Witman. 1979. Protein composition of the partition protofilaments of *Chlamydomonas* flagellar outer doublet microtubules. *J. Cell Biol.* 83: (2, Pt. 2):345 (Abstr.). *a*
24. Gibbons, I. R. 1961. The relationship between the fine structure and direction of beat in gill cilia of a lammellibranch mollusc. *J. Biophys. Biochem. Cytol.* 11:179–205.
25. Gibbons, I. R. 1965. Chemical dissection of cilia. *Arch. Biol.* 76:317–352.
26. Gibbons, I. R. 1975. The molecular basis of flagellar motility in sea urchin spermatozoa. *In* Molecules and Cell Movement. S. Inoue and R. E. Stephens, editors. Raven Press, New York. 207–232.
27. Gibbons, I. R. 1977. Structure and function of flagellar microtubules. *In* International Cell Biology, 1976–1977. B. R. Brinkley and K. R. Porter, editors. The Rockefeller University Press, New York. 348–357.
28. Gibbons, I. R., and A. V. Grimstone. 1960. On flagellar structure in certain flagellates. *J. Biophys. Biochem. Cytol.* 7:697–716.
29. Henley, C., D. P. Costello, M. B. Thomas, and W. D. Newton. 1969. The "9 + 1" pattern of microtubules in spermatozoa of *Mesostoma* (Platyhelminthes, Turbellaria). *Proc. Natl. Acad. Sci. U. S. A.* 64:849–856.
30. Hopkins, J. M. 1970. Subsidiary components of the flagella of *Chlamydomonas reinhardii*. *J. Cell Sci.* 7:823–839.
31. Horridge, G. A. 1965. Macrocilia with numerous shafts from the lips of the ctenophore *Beroe*. *Proc. R. Soc. Lond. B Biol. Sci.* 162:351–364.
32. Jacobs, M. J., J. M. Hopkins, and J. T. Randall. 1968. The flagellar proteins of a paralyzed mutant of *Chlamydomonas reinhardii*. *J. Cell Biol.* 39(2, Pt. 2):66 (Abstr.). *a*
33. Jacobs, M., and A. McVittie. 1970. Identification of the flagellar proteins of *Chlamydomonas reinhardii*. *Exp. Cell Res.* 63:53–61.
34. Kim, H., L. I. Binder, and J. L. Rosenbaum. 1979. The periodic association of MAP_2 with brain microtubules in vitro. *J. Cell Biol.* 80:266–276.
35. Kirschner, M. W. 1978. Microtubule assembly and nucleation. *Int. Rev. Cytol.* 54:1–71.
36. Klug, A., and D. J. DeRosier. 1966. Optical filtering of electron micrographs: reconstruction of one-sided images. *Nature (Lond.)*. 212:29–32.
37. Linck, R. W. 1973. Comparative isolation of cilia and flagella from the lammelibranch mollusc, *Aequipecten irradians*. *J. Cell Sci.* 12:345–367.
38. Linck, R. W. 1973. Chemical and structural differences between cilia and flagella from the lamellibranch mollusc, *Aequipecten irradians*. *J. Cell Sci.* 12:951–981.
39. Linck, R. W. 1976. Flagellar doublet microtubules: fractionation of minor components and α-tubulin from specific regions of the A-tubule. *J. Cell Sci.* 20:405–439.
40. Linck, R. W. 1976. Fractionation of minor component proteins and tubulin from specific regions of flagellar doublet microtubules. *In* Cell Motility. R. Goldman, T. Pollard, and J. Rosenbaum, editors. Cold Spring Harbor Laboratory, Cold Spring Harbor, New York. 869–890.
41. Linck, R. W. 1979. Advances in the ultrastructural analysis of the sperm flagellar axoneme. *In* The Spermatozoon. D. W. Fawcett and J. M. Bedford, editors. Urban and Schwarzenberg, Baltimore. 99–115.
42. Linck, R. W., and L. A. Amos. 1974. The hands of helical lattices in flagellar doublet microtubules. *J. Cell Sci.* 14:551–559.
43. Linck, R. W., and L. A. Amos. 1974. Flagellar doublet microtubules: selective solubilization of minor component proteins. *J. Cell Biol.* 63(2, Pt. 2):194 (Abstr.). *a*
44. Linck, R. W., and G. L. Langevin. 1981. Reassembly of flagellar B($\alpha\beta$) tubulin into singlet microtubules: consequences for cytoplasmic microtubule structure and assembly. *J. Cell Biol.* 89:323–337.
45. Little, M. 1979. Identification of a second β-chain in pig brain tubulin. *FEBS (Fed. Eur. Biochem. Soc.) Lett.* 108:238–286.
46. Ludueña, R. F., E. M. Shooter, and L. Wilson. 1977. Structure of the tubulin dimer. *J. Biol. Chem.* 252:7006–7014.
47. Mandelkow, E., J. Thomas, and C. Cohen. 1977. Microtubule structure at low resolution by x-ray diffraction. *Proc. Natl. Acad. Sci. U. S. A.* 74:3370–3374.
48. Mandelkow, E. M., E. Mandelkow, N. Unwin, and C. Cohen. 1977. Tubulin hoops. *Nature (Lond.)* 265:655–657.
49. Mandelkow, E. M., E. Mandelkow, and R. Schultheiss. 1979. Correlation between structural polarity and polar assembly of brain tubulin. *J. Mol. Biol.* 135:293–299.
50. McEwen, B., and S. J. Edelstein. 1980. Evidence for a mixed lattice in microtubules reassembled *in vitro*. *J. Mol. Biol.* 139:123–145.
51. McIntosh, J. R., E. S. Ogata, and S. C. Landis. 1973. The axostyle of *Saccinobaculus*. I. Structure of the organism and its microtubule bundle. *J. Cell Biol.* 56:304–323.
52. Meza, I., B. Huang, and J. Bryan. 1972. Chemical heterogeneity of protofilaments forming the outer doublets from sea urchin flagella. *Exp. Cell Res.* 74:535–540.
53. Mooseker, M. S., and L. G. Tilney. 1973. Isolation and reactivation of the axostyle. Evidence for a dynein-like ATPase in the axostyle. *J. Cell Biol.* 56:13–26.
54. Murphy, D. B., and G. G. Borisy. 1975. Association of high-molecular-weight proteins with microtubules and their role in microtubule assembly *in vitro*. *Proc. Natl. Acad. Sci. U. S. A.* 72:2696–2700.
55. Nakamura, S., and R. Kamiya. 1978. Bending motion in split flagella of *Chlamydomonas*. *Cell Struct. Funct.* 3:141–144.
56. Olson, G. E., and R. W. Linck. 1977. Observations on the structural components of flagellar axonemes and central pair microtubules from rat sperm. *J. Ultrastruct. Res.* 61: 21–43.
57. Olson, G. E., and R. W. Linck. 1980. Membrane differentiations in spermatozoa of the squid, *Loligo pealeii*. *Gamete Res.* 3:329–342.
58. Omoto, C. K., and C. Kung. 1980. Rotation and twist of the central-pair microtubules in the cilia of *Paramecium*. *J. Cell Biol.* 87:33–46.
59. Perotti, M. E. 1969. Ultrastructure of the mature sperm of *Drosophila melanogaster* meig. *J. Submicrosc. Cytol.* 1:171–195.
60. Phillips, D. M. 1974. Structural variants of invertebrate sperm flagella and their relationship to motility. *In* Cilia and Flagella. M. A. Sleigh, editor. Academic Press, Inc., New York. 379–401.
61. Prensier, G., E. Vivier, S. Goldstein, and J. Schrevel. 1980. Motile flagellum with a "3 + 0" ultrastructure. *Science (Wash. D.C.)*. 207:1493–1494.
62. Rosenthal, E. T., and R. W. Linck. 1979. Sequential regulation of doublet microtubule sliding in demembranated rat sperm models. *J. Cell Biol.* 83(2, Pt. 2):181 *a* (Abstr.).
63. Sandoval, I. V., and K. Weber. 1979. Polymerization of tubulin in the presence of colchicine or podophyllotoxin. Formation of a ribbon structure induced by guanylyl-5′-methylene diphosphonate. *J. Mol. Biol.* 134:159–172.
64. Satir, P. 1965. Studies on cilia. II. Examination of the distal region of the ciliary shaft and the role of the filaments in motility. *J. Cell Biol.* 26:805–834.
65. Satir, P. 1968. Studies on cilia. III. Further studies on the cilium tip and a "sliding filament" model of ciliar motility. *J. Cell Biol.* 39:77–94.
66. Shay, J. W. 1972. Electron microscope studies of spermatozoa of *Rhynchosciara* sp. I. Disruption of microtubules by various treatments. *J. Cell Biol.* 54:598–608.
67. Shelanski, M. L., and E. W. Taylor. 1968. Properties of the protein subunit of central-pair and outer doublet microtubules of sea urchin flagella. *J. Cell Biol.* 38:304–315.
68. Stephens, R. E. 1975. High-resolution preparative SDS polyacrylamide gel electrophoresis: fluorescent visualization and electrophoretic elution-concentration of protein bands. *Anal. Biochem.* 65:369–379.
69. Stephens, R. E. 1978. Primary structural differences among tubulin subunits from flagella, cilia, and the cytoplasm. *Biochemistry* 17:2882–2891.
70. Stephens, R. E. 1979. Equimolar heterodimers in microtubules? *J. Cell Biol.* 83(2, Pt. 2): 351 *a* (Abstr.).
71. Sullivan, K. F., K. W. Farrell, and L. Wilson. 1979. Developmental analysis of chick brain tubulin heterogeneity. *J. Cell Biol.* 83(2, Pt. 2):351 *a* (Abstr.).
72. Summers, K. E., and I. R. Gibbons. 1971. Adenosine-triphosphate-induced sliding of tubules in trypsin-treated flagella of sea urchin sperm. *Proc. Natl. Acad. Sci. U. S. A.* 68: 3092–3096.
73. Tamm, S. L. 1979. Ionic and structural basis of ciliary reversal in ctenophores. J. Cell Biol. 83(2, Pt. 2):174 *a* (Abstr.).
74. Tamm, S. L., and G. A. Horridge. 1970. The relation between the orientation of the central fibrils and the direction of beat in cilia of *Opalina*. *Proc. R. Soc. Lond. B Biol. Sci.* 175: 219–233.
75. Tilney, L. G., J. Bryan, D. J. Bush, K. Fujiwara, M. S. Mooseker, D. B. Murphy, and D. H. Snyder. 1973. Microtubules: evidence for 13 protofilaments. *J. Cell Biol.* 59:267–275.
76. Warner, F. D. 1970. New observations on flagellar fine structure. The relationship between matrix structure and the microtubule component of the axoneme. *J. Cell Biol.* 47:159–182.
77. Warner, F. D. 1974. The fine structure of the ciliary and flagellar axoneme. *In* Cilia and Flagella. M. A. Sleigh, editor. Academic Press, Inc., New York. 11–37.
78. Warner, F. D. 1976. Ciliary inter-microtubule bridges. *J. Cell Sci.* 20:101–114.
79. Warner, F. D., and P. Satir. 1974. The structural basis of ciliary bend formation. Radial spoke positional changes accompanying microtubule sliding. *J. Cell Biol.* 63:35–63.
80. Witman, G. B., K. Carlson, J. Berliner, and J. L. Rosenbaum. 1972. *Chlamydomonas* flagella. I. Isolation and electrophoretic analysis of microtubules, matrix, membranes, and mastigonemes. *J. Cell Biol.* 54:507–539.
81. Witman, G. B., K. Carlson, and J. L. Rosenbaum. 1972. *Chlamydomonas* flagella. II. The distribution of tubulins 1 and 2 in the outer doublet microtubules. *J. Cell Biol.* 54:540–555.
82. Witman, G. B., J. Plummer, and G. Sander. 1978. *Chlamydomonas* flagellar mutants lacking radial spokes and central tubules. Structure, composition, and function of specific axonemal components. *J. Cell Biol.* 76:729–747.
83. Woodrum, D. T., and R. W. Linck. 1980. The structural basis of motility in the microtubular axostyle: implications for cytoplasmic microtubule structure and function. *J. Cell Biol.* 89:404–414.